

Journal of Materials Chemistry A

Accepted Manuscript



This is an *Accepted Manuscript*, which has been through the Royal Society of Chemistry peer review process and has been accepted for publication.

Accepted Manuscripts are published online shortly after acceptance, before technical editing, formatting and proof reading. Using this free service, authors can make their results available to the community, in citable form, before we publish the edited article. We will replace this *Accepted Manuscript* with the edited and formatted *Advance Article* as soon as it is available.

You can find more information about *Accepted Manuscripts* in the [Information for Authors](#).

Please note that technical editing may introduce minor changes to the text and/or graphics, which may alter content. The journal's standard [Terms & Conditions](#) and the [Ethical guidelines](#) still apply. In no event shall the Royal Society of Chemistry be held responsible for any errors or omissions in this *Accepted Manuscript* or any consequences arising from the use of any information it contains.

Cite this: DOI: 10.1039/c0xx00000x

www.rsc.org/Materials

PAPER

Polyimide nanocomposites with boron nitride-coated multi-walled carbon nanotubes for enhanced thermal conductivity and electrical insulation

Wei Yan,^{ab} Yi Zhang,^{*a} Huawei Sun,^a Siwei Liu,^a Zhenguo Chi,^a Xudong Chen^a and Jiarui Xu^a

Received (in XXX, XXX) Xth XXXXXXXXX 20XX, Accepted Xth XXXXXXXXX 20XX

DOI: 10.1039/b000000x

Polyimide nanocomposites with boron nitride-coated multi-walled carbon nanotubes (BN-c-MWCNTs) were successfully prepared with enhanced thermal conductivity and electrical insulation. The inorganic BN nano-layer on the MWCNTs surface provides electrical insulation and prevents the formation of MWCNTs electrically conductive networks in the PI matrix. The BN-c-MWCNTs/PI films exhibited synchronously good thermal conductivity and relatively high electrical resistivity. Compared with that of pure PI, the thermal conductivity of the BN-c-MWCNTs/PI films with 3 wt.% BN-c-MWCNTs increased by 106%. In addition, the electrical insulation of the BN-c-MWCNTs/PI films was also improved compared with that of the MWCNTs/PI composite films. All the above-mentioned properties provide advantages to the PI hybrid films in electronic packaging and electrical insulation.

Introduction

The discovery of carbon nanotubes (CNTs) has attracted substantial interests because of their unique mechanical, thermal, and electronic properties.¹ However, the application of CNTs has been limited to the field of electronic packaging and electrical insulation due to their excellent electrical conductivity. In addition, the low thermal conductivity enhancement of CNT composites has been mainly attributed to the high interfacial thermal resistance between CNTs and the polymer matrix, high tube-tube contact resistance, structural defects of CNTs, small contact area between CNTs, as well as resonant coupling between the CNTs and the surrounding matrices.²⁻⁹ Boron nitride (BN) has low density, high thermal conductivity, and is chemically inert. Particularly, BN has received significant attention because it provides to be insulation, non-reactive to molten metal, and having a higher oxidation resistance than carbon.¹⁰⁻¹² Thus, combining the advantages of these two materials would be favourable for the design of nanoscale electronic devices and

nanostructure composites. Our research group has performed studies on the surface modification of CNTs by using insulating inorganic layers, such as AlO(OH)-coated MWCNTs.¹³ This strategy has been proved to be a worthy method for improving the thermal conductivity and insulation of polymer films. There are several research results concerning BN-coated CNTs. Chen¹⁴ reported a method to coat BN on CNTs via a reaction between boric acid and ammonia at 1100–1200 °C. Yoo¹⁵ prepared BN films on CNTs by reactive sputtering. However, the methods available to synthesize BN-coated CNTs have the disadvantages of complicated apparatus and high temperature, resulting in the increase of production cost. Furthermore, high temperature will damage the surface of CNTs.

Polyimide (PI) is widely used in microelectronics and aerospace industries as the materials for electronic packaging and electrical insulation because of their excellent thermal stability, mechanical properties, and low dielectric constants.^{16,17} When operating a microelectronic product, a considerable amount of heat is generated, which must be dissipated to avoid overheating.¹⁸ This fact suggests that the insulating or packaging materials should possess good thermal conductivity, in addition to the traditionally desired physical-mechanical properties. To address the heat dissipation dilemma, ceramic fillers, such as alumina,¹⁹⁻²² silica,^{23,24} silicon carbide,²⁵ silicon nitride,²⁶⁻²⁸ aluminum nitride,²⁹⁻³⁵ and BN³⁶⁻⁴² have been used as the thermal conductive components embedded in the polymer matrices. The conventional method used to fabricate thermally conductive composites was performed by utilizing different filler-type mixtures to form a thermally conductive network.^{43,44} However, this method required a high solid loading in order to form thermally conductive networks, and the physical-mechanical properties of the polymer composites were consequently limited.

^aPCFM lab, DSAPM Lab, GD HPPC Lab, State Key Laboratory of Optoelectronic Materials and Technologies, School of Chemistry and Chemical Engineering, Sun Yat-sen University, Guangzhou 510275, PR China

Fax: +86 20 84112222; Tel: +86 20 84112222;

E-mail: ceszy@mail.sysu.edu.cn

^bEngineering Technology Research Center for Materials Protection of Wear and Corrosion of Guizhou Province, College of Chemistry and Materials Engineering, Guiyang University, Guiyang, 550025, PR China.

†Electronic Supplementary Information (ESI) available: TEM and SEM images of boron nitride, the effect of filler content on the electrical resistivity and thermal conductivity of polyimides. See DOI: 10.1039/b000000x/

In this study, a novel approach to fabricate thermally conductive and insulated PI nanocomposites through the surface modification of MWCNTs has been developed. The aim is to investigate the formation of the inorganic BN nanolayer on the MWCNT surface through thermal treatment. A simple and effective method was performed to prepared BN-c-CNTs, where boric acid and urea were used as precursor, and a much lower temperature (900 °C) was used, which can effectively avoid the consumption and destruction of carbon layers. The BN nanolayer on MWCNT surfaces is an insulated thermally conductive inorganic material that can prevent the formation of electrically conductive carbon nanotube networks in the PI matrix. Moreover, the BN-c-MWCNTs can provide excellent thermal conductivity properties to MWCNTs through our special coating technology. This method could substantially improve the dispersion of the modified MWCNTs into the solvent and the PI matrix. To the best of our knowledge, thermally conductive and insulated PI nanocomposite films based on BN coated onto the MWCNTs surface are rarely reported in the literature.

Experimental

Materials

MWCNT samples with grade NC7000 from Nanocyl (mean diameter: 9.5 nm, purity: 90%) were used in the coating experiments. Their BET specific surface, which was 250–300 m² g⁻¹, was calculated using nitrogen absorption. Boric acid and nitric acid were purchased from Guangzhou Chemical Reagent Co., Ltd. Urea ((NH₂)₂CO, AR) was purchased from Shantou Xilong Chemical Reagent Co., Ltd., China. Both 3,3',4,4'-biphenyltetracarboxylic dianhydride (BPDA) and 4,4'-oxydianiline (ODA) were purchased from Allstar Tech. (Zhongshan) Co., Ltd., Zhongshan, GD, China. 4,4'-Diaminodiphenyl sulfide (SDA) was purchased from Shou & Fu Chemical Co., Ltd., Zhejiang, China. N,N-Dimethylformamide (DMF) with analytical purity was purchased from Guangzhou Chemical Reagent Factory, Guangdong, China. Other solvents and compounds were purchased from Guangzhou Chemical Reagent Co., Ltd.

Synthesis

Functionalization of MWCNTs. About 2 g of the as-received MWCNTs were dispersed in 200 mL of 68% nitric acid in a 500 mL round bottom flask equipped with a condenser. The dispersion was refluxed at 110 °C for 8 h. Afterward, the resulting dispersion was diluted with water and filtered. The residual solid was washed until neutral pH, dried in vacuum at 100 °C overnight, cooled to room temperature, and then stored in a desiccator, marked as f-MWCNTs.

Preparation of BN-c-MWCNTs. BN-c-MWCNTs were prepared via a direct impregnation technique. The functionalized MWCNTs (f-MWCNTs, 1 g) and absolute ethyl alcohol (160 mL) were poured into a 500 mL round bottom flask and sonicated for 1 h at room temperature. Afterward, H₃BO₃ (16 g) particles were added and sonicated for 0.5 h. When H₃BO₃ dissolved, urea (100 g) was dispersed in the solution with high ultrasonication for 0.5 h. The solution was then magnetically stirred at high speed for 12 h at room temperature. The solution was filtered through a PTFE membrane (0.45 μm). The resulting fluffy black powder was dried in a vacuum drying chamber at 40 °C for at least 12 h. The mixed powder was removed, loaded

in a quartz boat, and placed into a horizontal quartz tube furnace. Before each experimental run, the furnace was purged with nitrogen for at least 30 min. The furnace was then heated to the desired operating temperature at a rate of 5 °C/min with ammonia flowing into the reaction tube at a flow rate of 200 mL/min. The sample was treated at 900 °C for 3 h and then cooled in the furnace under ammonia flow for protection.

Preparation of MWCNT/PI and BN-c-MWCNT/PI composite films. A series of MWCNT/PAA and BN-c-MWCNT/PAA solutions were prepared via an in situ polymerization process with sonication and MWCNT or BN-c-MWCNT concentrations ranging from 0 to 3.0 wt.%. The method was as follows: MWCNTs or BN-c-MWCNTs were pretreated with DMF under ultrasonication and mechanical agitation to uniformly disperse them in the solution under argon. The diamine monomer ODA and SDA (ODA:SDA = 3:1) were then added into the MWCNTs/DMF or BN-c-MWCNTs/DMF suspension with ultrasonication and mechanical stirring. After the diamine monomers were completely dissolved, BPDA was partially added into the above system, and the total mole ratio of the diamine to the dianhydride was 0.995:1.0. The solid content of the in situ synthesized MWCNT/PAA or BN-c-MWCNT/PAA solution was 18 wt.%. The whole mixture was mixed with ultrasonication and mechanical stirring at room temperature for 8 h.

The homogeneous and viscous MWCNT/PAA and BN-c-MWCNT/PAA solutions were casted onto a clean glass plate and then dried in an air-circulating oven at 100 °C for 0.5 h to volatilize the DMF solvent. The nanocomposite films were imidized by heating the composite film in a high temperature vacuum oven at 150 °C, 250 °C, and 350 °C for 0.5 h at each respective temperature. The thickness of the PI films were ca 40 μm.

Characterization and instruments

Field emission scanning electron microscopy (FE-SEM; Japan; s4800) was used to confirm the morphologies of the MWCNTs/PI and BN-c-MWCNTs/PI composite films. The samples were sputtered with a thin layer of platinum to prevent charge accumulation before the FE-SEM observation. The morphologies of the MWCNTs and BN-c-MWCNTs were characterized via high-resolution transmission electron microscopy (HRTEM, FEI Tecnai G2 F30) at an accelerating voltage of 300 kV. X-ray photoelectron spectroscopy (XPS) was used to determine the chemical composition of the BN-c-MWCNTs surface. XPS spectra were obtained using an ESCALAB 250 spectrometer operated in a fixed analyser transmission mode (pass energy 150 eV) and Al-K irradiation (1486.6 eV) excitation. The spectra were referenced to the C1s line of the hydrocarbon-type carbon set with a binding energy of 284.6 eV. All XPS spectra and peak area intensity data were obtained via Shirley-type background subtraction. The crystal structure was characterized via X-ray diffraction (XRD, Bruker D8) with Cu-Kα radiation (λ = 1.54051 Å). Step scanning was used with 2θ intervals from 10° to 80° and a residence time of 1 s. The thermal diffusivity (α, mm² s⁻¹) at room temperature was measured on disk samples via the laser flash method (Netzsch Instruments Co., Nanoflash LFA 447 system). The specific heat (C_p, J g⁻¹ K⁻¹) at room temperature was measured on disk samples via differential scanning calorimetry (DSC, Perkin-Elmer Co., DSC-8500), and the bulk density (ρ, g cm⁻³) of the specimens was measured via the water displacement method (Alfa Mirage Co. Ltd., Electronic Densimeter SD-200L). For each measurement, five samples were tested three times. The thermal

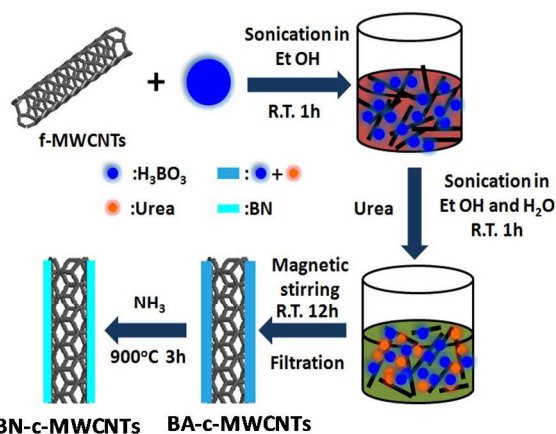
conductivity (λ , $\text{W m}^{-1}\text{K}^{-1}$) was calculated using the following equation:

$$\lambda = c_p \cdot \rho \cdot \alpha$$

The resistance parameters, such as the volume resistivity (R_v) and surface resistivity (R_s), were determined using an Agilent 4339B high-resistance meter (Agilent Technologies Japan, Ltd.). Dynamic mechanical analysis (DMA) of the PI composite films was performed from 50 °C to 400 °C by using a TA instrument Q800 analyzer at a heating rate of 3 °C/min and a frequency of 1 Hz. The storage modulus and $\tan \delta$ were measured, and T_g was determined from the peak temperature of the $\tan \delta$ curves. Thermomechanical analysis (TMA, Q400, TA Instruments) was conducted in extension mode with a tension force of 0.05 N at a heating rate of 5 °C min^{-1} and a frequency of 1 Hz under nitrogen. Coefficient of thermal expansion (CTE) was evaluated using the TMA data from 100 °C to 200 °C, which is a commonly applied test condition in manufacturing. The tensile strength and modulus of the nanocomposites were measured using a Shenzhen SANS machine Model CMT 6103 at room temperature via the ASTM-D882 test method. The test samples were cut into strips with a size of 100 mm \times 10 mm \times 0.04 mm. The gauge length was 50 mm, and the cross-head speed was maintained at 2 mm/min. The mechanical properties were evaluated using the built-in software of the machine. A minimum of five tests were performed for each composite sample, and their average was reported.

Results and discussion

Surface modification of MWCNTs by boron nitride was carried out by a direct impregnation technique. Firstly, pure MWCNTs were oxidized in nitric acid. This process causes a continuous increase of the defective sites and generates functional groups, such as -OH and -COOH on the surface of MWCNTs (Fig. S1 in the Supplementary Information), thus increases the reactivity of MWCNTs. Then, the f-MWCNTs were well dispersed in absolute ethyl alcohol by ultrasonic. After that, H_3BO_3 and urea particles were added respectively. And H_2O was also added in order to dissolve the urea. To finished the impregnation process, the system was mixed for 0.5 h under ultrasonic condition, and for another 12 h under stirring. Finally, the boric acid and urea wrapped MWCNTs (BA-c-MWCNTs) was filtrated and heated at 900 °C for 3 h in NH_3 to formed the boron nitride coating. The processing of the preparation of BN-c-MWCNTs was shown in Scheme 1.



Scheme 1. outline of the preparation of the BN-c-MWCNT.

The morphologies of MWCNTs and BN-c-MWCNTs were examined by TEM, the results are shown in Fig. 1. As can be

seen, the surface of the initial MWCNTs is smooth, with a diameter of about 10 nm and a wall thickness of about 3 nm (Fig. 1a). A small quantity of impurities was detected on the surfaces of the nanotubes that are produce residues, such as amorphous carbon and catalytic residues. After oxidation, the surface of the f-MWCNTs became rough with some curvatures or defects on it (as shown in red arrow in Fig. 1b). After surface modification, as shown in Fig. 1c, the surface of the MWCNTs were well covered with a thin layer of about 3 nm with a lamellar structure, which suggests that BN was successfully coated onto the carbon nanotube surface via the described high-temperature method under NH_3 atmosphere.

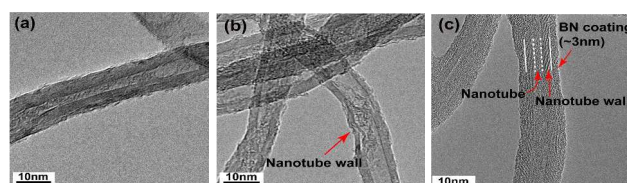


Fig. 1. TEM images of MWCNTs: (a) pure MWCNTs, (b) f-MWCNTs, and (c) BN-c-MWCNTs.

XRD analyses were used to study the crystalline structures of the MWCNTs and coating, as shown in Fig. 2. The XRD pattern of the as-synthesized BNs shows reflection peaks at $2\theta = 25.8^\circ$ and 42.2° (Fig. 1), which coincide with the Bragg angles of (0 0 2) and (1 0 0) in hexagonal BN.⁴³ Its TEM image indicates the presence of a turbostratic structure (Fig. S2 in the Supplementary Information). The characteristic diffraction peaks of f-MWCNTs exhibits at $2\theta = 25.6^\circ$ and 42.8° (Fig. 2). The structure of BN seems similar to that of MWCNTs. For the BN-c-MWCNTs, the diffraction peaks show at $2\theta = 26.0^\circ$ and 42.8° . Compared with f-MWCNTs, the diffraction angle at $2\theta = 25.8^\circ$ shifts to a higher value (26.0°) with some asymmetry owing to the coating with BN, and no diffractions of other BCN compounds was detected.⁴⁵ The diffraction peak asymmetry can be ascribed to the superposition of the (0 0 2) planes of BN and carbon.¹⁴ In addition, the reflection peaks at about $2\theta = 53.6^\circ$ and 78.3° indicate that the coating layer was a BN superstructure.⁴⁶ Consequently, the results demonstrate that the BN layer was successfully coated onto the MWCNT surface.

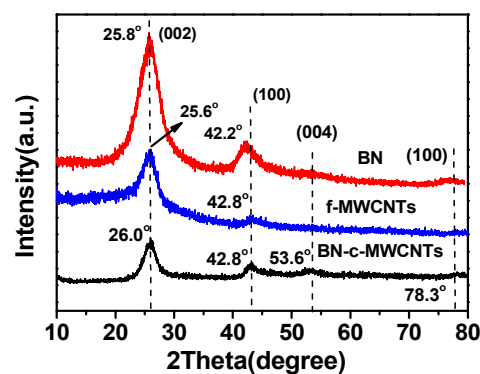


Fig. 2 XRD patterns of the as-synthesized BN, f-MWCNTs and BN-c-MWCNTs.

XPS was used to identify the compositional information of the coating. The wide scan XPS spectrum of the BN-c-MWCNTs in Fig. 3a reveals the presence of boron, carbon, nitrogen, and oxygen. The deconvoluted B1s, C1s and N1s and peak fitting are shown in Fig. 3b-d. B1s spectrum (Fig. 3b) has the peaks at

191.0 and 189.9 eV, corresponding to the B-N and B-C bonding, respectively. In addition, the peak at 192.1 eV indicates the existence of oxynitrides (BO_xN_y) with B_2O_3 species in the coating caused by the incomplete reaction of boric acid and urea in NH_3 at low reaction temperatures (900 °C).⁴⁷ From these results, the reaction of ammonia with boric acid and urea on MWCNTs leads to the formation of BN nanolayer. The curve-fitted C 1s spectrum (Fig. 3c) shows two main peaks centered at 284.8 and 285.8 eV, which are ascribed to C-C and C-N, respectively.^{48–50} The fitted N 1s spectra present two peaks centered at 398.4 and 398.9 eV (Fig. 3d). The former is assigned to the N-B bonding and the latter to the N-C bonding.⁵¹ Consequently, by combining the TEM, XRD and XPS results, we concluded that BN coatings were successfully prepared on the surface of MWCNTs via the direct impregnation process. Meanwhile, the surface modification of MWCNTs by BN brings rich hydroxyl group on the surface of the nano-fillers (Fig. 4), which may improve the distribution of BN-c-MWCNTs in the polymer matrix.

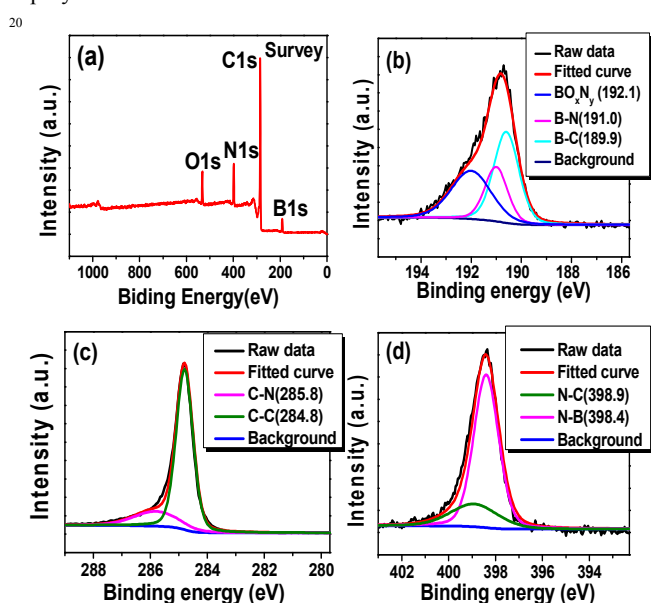


Fig. 3. XPS spectra of the BN-c-MWCNTs: (a) XPS wide-scan; (b) B1s; (c) C1s; and (d) N1s high-resolution spectra of BN-c-MWCNTs.

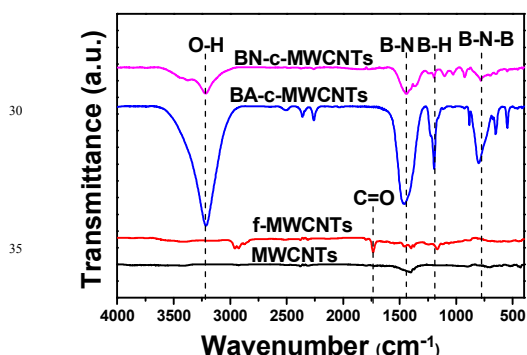
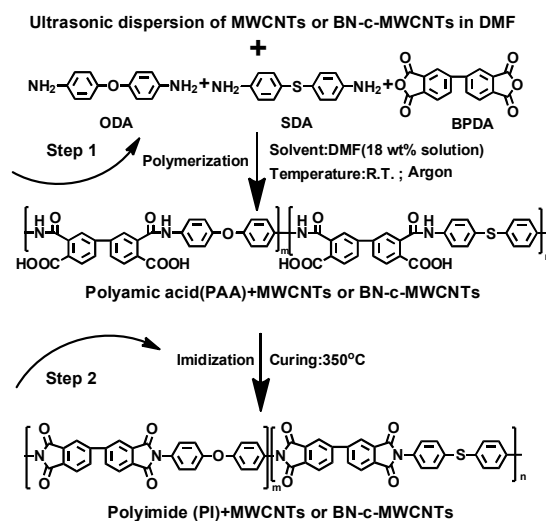


Fig. 4. FTIR spectra of MWCNTs, f-MWCNTs, BA-MWCNTs and BN-c-MWCNTs.

Polyimide was prepared using BPDA as diacid, ODA and SDA with a ratio of 3:1 as diamine, which were chosen based on our previous work, aiming at the adhesion between polyimide and copper.^{52–53} MWCNTs/PI and BN-c-MWCNTs/PI

nanocomposite films were prepared via a two-step process, as shown in Scheme 2. At the first step, MWCNTs and BN-c-MWCNTs were pretreated in DMF under ultrasound and mechanical agitation. Then a series of MWCNTs/PAA and BN-c-MWCNTs/PAA solutions were prepared using an *in situ* polymerization process under sonication with different MWCNTs or BN-c-MWCNTs concentrations. In step 2, the viscosity composite PAA solutions were cast onto clean, dry plate glass, followed by a thermal imidization process at high temperature. The thickness of the films were ca 40 μm . Fig. 5 shows the pictures of the pure PI film, the MWCNTs/PI film with 1.0 wt% MWCNTs content and the BN-c-MWCNTs/PI film with 3.0 wt% BN-c-MWCNTs content. The pure PI film is greenish-yellow, the MWCNT/PI film is black, however, the color of the BN-c-MWCNT/PI film is similar to the pure PI and was transparent when the BN-c-MWCNT content reached 3 wt.%.



Scheme 2. Preparation of the PI nanocomposite films via an *in situ* polymerization process.

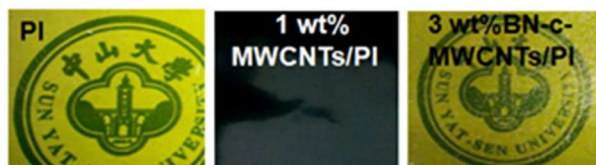


Fig. 5. Photographs of PI nanocomposite films.

To investigate the dispersion of MWCNTs and BN-c-MWCNTs in the PI matrix, the composite films were dipped into liquid nitrogen and then broken. The FE-SEM images of the fracture surfaces of the neat PI and the PI composites with nanotubes contents of 1 and 3 wt.% are shown in Fig. 6. The fracture surface of the pure PI was homogeneous and smooth (Figs. 6a–b). In the SEM images of MWCNTs/PI and BN-c-MWCNTs/PI with a content of 1 wt.%, the fillers were tightly embedded in the films, which suggests the excellent compatibility and homogeneity of the composite films (Fig. 6c–d). Furthermore, Fig. 6e shows that although the nanotubes exhibit a high degree of dispersion throughout the PI matrix for MWCNT fillers, they were also occasionally pulled out from the PI matrix (as shown by the arrow). Although the random orientation of BN-c-MWCNTs was in the selected section, BN-c-MWCNTs were also embedded in the PI matrix, as shown in Fig.

6f, and the nanotubes are broken on the surface (indicated by the arrows), which suggests strong polymer-nanotube interfacial adhesion and a thick cladding of polymer on the nanotube surface. Moreover, this finding implies that thermal conductive fillers were dispersed well in the PI-precursor solution, which is extremely important for the improving of the thermal conductivity of the composite films. Therefore, the *in situ* polymerization process provides good compatibility and dispersion of MWCNTs in the matrix and is an effective approach to enhance the reinforcing efficiency of MWCNTs and provide superior composite performance.

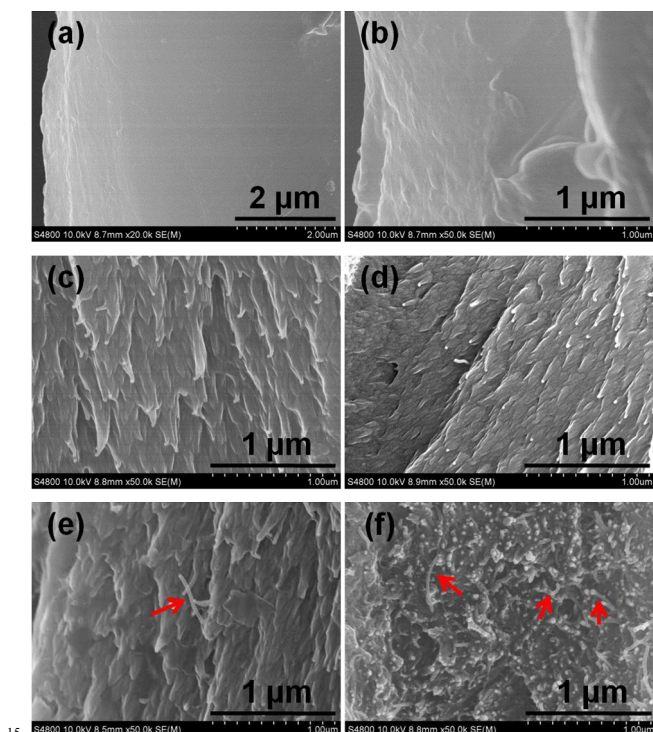


Fig. 6. FE-SEM images of fractured surface of PI composite films: (a) Neat PI ($\times 20k$); (b) Neat PI ($\times 50k$); (c) 1 wt.% MWCNTs; (d) 1 wt.% BN-c-MWCNTs; (e) 3 wt.% MWCNTs; and (f) 3 wt.% BN-c-MWCNTs.

Table 1. Mechanical properties of the MWCNT/PI and BN-c-MWCNT nanocomposite films^a.

Sample	Content (wt.%)	Tensile Strength (MPa)	Tensile Modulus (GPa)	Elongation At break (%)
Neat-PI	0	102.5 \pm 6.4	2.2 \pm 0.3	4.3 \pm 3.6
MWCNT/PI	0.1	133.7 \pm 7.3	3.1 \pm 0.2	8.5 \pm 2.3
	1	134.1 \pm 5.8	3.0 \pm 0.5	8.7 \pm 1.3
	3	135.6 \pm 8.4	3.0 \pm 0.2	7.3 \pm 3.4
BN-c-MWCNT/PI	0.1	120.9 \pm 9.4	2.3 \pm 0.3	7.0 \pm 4.2
	1	121.8 \pm 7.6	2.0 \pm 0.5	8.2 \pm 3.2
	3	131.9 \pm 6.8	2.5 \pm 0.4	6.3 \pm 4.4

^aResults were obtained from data average for five samples. Standard deviation of obtained results was below 5%.

Table 1 shows the mechanical properties of the PI nanocomposite films. Compared with pure PI, the tensile properties of the nanocomposites increase upon the incorporating

of MWCNTs and BN-c-MWCNTs. The tensile modulus and strength of neat PI films is 2.21 GPa and 102.5 MPa, respectively. The tensile strength improved by about 32% from 102.5 MPa to 135.6 MPa, and the tensile modulus improved by about 37% from 2.21 GPa to 3.02 GPa when the loading of the MWCNTs was 3 wt.%. The best mechanical properties of the BN-c-MWCNT/PI nanocomposite films were achieved by incorporating 3 wt.% BN-c-MWCNTs, and the tensile strength improved from 102.5 MPa to 131.9 MPa. Moreover, the tensile modulus improved from 2.21 GPa to 2.47 GPa.

Table 2 summarizes the thermal properties of the composite films. The glass transition temperature (T_g) of the composite films are higher than that of the neat PI. The materials become more elastic because the damping peak occurs in the glass transition region and the $\tan \delta_{max}$ can be identified as the T_g . This result indicates that the nanofillers can increase the T_g of the PI matrix. The neat PI exhibited high thermo-oxidative stability. The thermo-oxidative decomposition behavior of the PI nanocomposites were similar to that of neat PI but showed higher decomposition temperature, which indicates that the addition of MWCNTs or BN-c-MWCNTs would improve the thermal stability of the PI nanocomposites. The coefficient of thermal expansion (CTE) of the PI composite films decreased with increasing the amounts of nanofillers. The CTE of the pristine PI film was 40.7 $\mu\text{m}/\text{m}^\circ\text{C}$, while that of the BN-c-MWCNTs/PI composite slightly decreased to 37.5 $\text{ppm}/^\circ\text{C}$ when the filler content is 0.1 wt.%. For the composite films, CTE is dependent on each component phase and the interactions between each phase.⁵⁴ Hence, the substantial decrease in CTE of PI films should originate from the adequate dispersion and interfacial physical bonds between the nanofillers and the PI matrix. The nanofiller can restrain the mobility of the loose molecular bonds in polymer chains as the temperature increases.

Table 2. Thermal properties of the MWCNT/PI and BN-c-MWCNT/PI nanocomposite films

Sample	Content (wt.%)	T_g ($^\circ\text{C}$) ^a	CTE ($\text{ppm}/^\circ\text{C}$) ^b	$T_{d5\%}$ ($^\circ\text{C}$) ^c
Neat-PI	0	283.9	40.7	537.9
MWCNTs/PI	0.1	290.7	40.3	541.7
	1	290.4	38.5	551.3
	3	290.8	37.7	568.5
BN-c-MWCNTs/PI	0.1	285.2	37.5	559.2
	1	291.8	37.8	558.9
	3	291.1	38.1	576.4

^a T_g : glass transition temperature, identified by DMA

^bCTE: coefficient of thermal expansion, measured by TMA determined over range of 100 $^\circ\text{C}$ to 200 $^\circ\text{C}$

^c $T_{d5\%}$: thermal decomposition temperature at 5% weight loss as determined by TGA.

MWCNTs have a high aspect ratio and π -bonds. Electrons are transferred through the π -bonds of CNTs. The addition of a small amount of CNT will significantly reduce the surface and volume of the electrical resistivity. Both the volume and surface resistances of the PI composite films were measured at room temperature, and the results are presented in **Fig. 7**. The plots show that the addition of MWCNTs or BN-c-MWCNTs into PI reduced the surface and volume resistances. **Fig. 7a** shows that with 3 wt.% MWCNT or BN-c-MWCNT loading, the volume resistances of the PI nanocomposite films were $6.82 \times 10^7 \Omega \text{ cm}$

and $7.69 \times 10^9 \Omega \text{ cm}$, respectively, while that of pure PI was $3.77 \times 10^{14} \Omega \text{ cm}$. **Fig. 7b** shows that the surface resistances of the composite films decreased from $1.17 \times 10^{13} \Omega \text{ cm}$ (pure PI) to $2.31 \times 10^7 \Omega \text{ cm}$ and $3.82 \times 10^9 \Omega \text{ cm}$ for MWCNTs/PI or BN-c-MWCNTs/PI respectively, when the filler loading was 3 wt.%. This result suggests that although the surface and volume resistances of the filled PI films are decreased, the values of resistances for the modified MWCNTs/PI films are about three orders of magnitude higher than those of non-modified ones, which is in the range of accepted properties for electronic packaging and/or electrical insulation materials. This can be due to that the surface modification of the MWCNTs through an inorganic insulating layer may effectively prevent the formation of MWCNTs electrically conductive networks in the PI matrix.

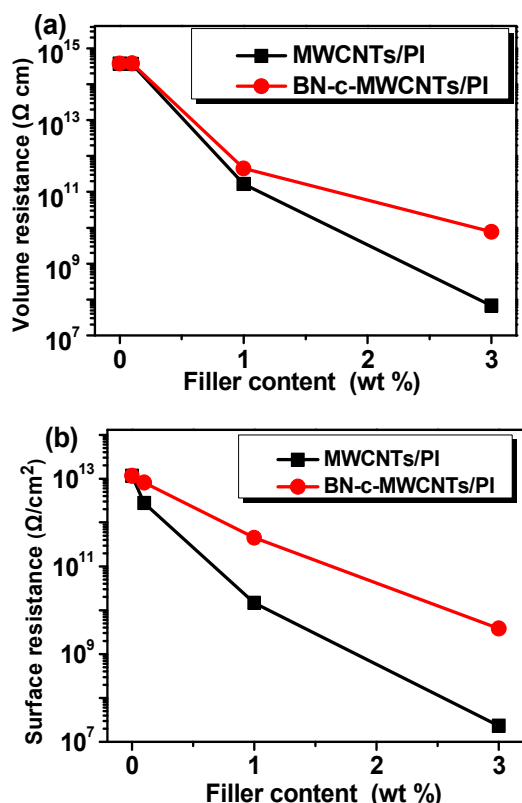


Fig. 7. Effect of filler content on electrical resistivity of PI nanocomposite films: (a) volume resistivity and (b) surface resistivity.

The thermal diffusivity and conductivity, density, specific heat capacity of the composite films are shown in **Table S2** in the Supplementary Information. **Fig. 8** shows the effect of the fillers on the thermal conductivities of the PI matrix. As can be seen, the thermal conductivity of the pure polyimide was $0.188 \text{ W m}^{-1}\text{K}^{-1}$. The thermal conductivity of the MWCNTs/PI composite films was firstly increased and reached the highest value ($0.306 \text{ W m}^{-1}\text{K}^{-1}$, **Fig. 8a**) when the content of MWCNTs was 0.1 wt%, which increased by about 60 % percent compared with pure PI (**Fig. 8b**). When the MWCNTs fraction was higher than 0.1wt%, the thermal conductivity of the PI films decreased but still higher than that of pure PI. That's because the dispersion of the as-received MWCNTs in the polyimide is quite poor; the aggregation of MWCNTs happens when its content is higher than

1 wt.%, which will directly affect the formation of the thermal conductive networks of MWCNTs in the matrix. For the BN-c-MWCNTs/PI systems, the thermal conductivity of the films increased with increasing the BN-c-MWCNTs content. When the content of BN-c-MWCNTs was 3 wt%, the thermal conductivity increased to around $0.388 \text{ W m}^{-1}\text{K}^{-1}$, which increased by about 106 % compared with that of pure PI (**Fig. 8b**), and the enhancement was almost 5 times of that of MWCNTs/PI system.

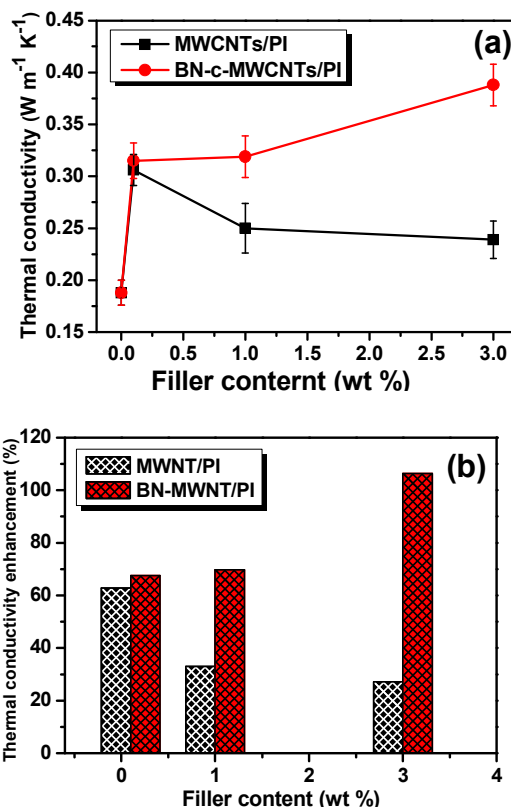


Fig. 8. Effect of filler content on the thermal conductivities of MWCNTs/PI and BN-c-MWCNTs/PI composite films.

The improvement of BN-c-MWCNTs to the thermal conductivity of the polyimide matrix can be attributed to the following reasons: (1) the high thermal conductivity of MWCNTs and BN, which is $2800 \text{ W m}^{-1}\text{K}^{-1}$ and $300 \text{ W m}^{-1}\text{K}^{-1}$, respectively; (2) through the direct impregnation technique, the morphology of the BN can be changed from traditional particle to nano-layer, according to the shape of the MWCNTs, which may effectively improve the aspect ratio of BN, thus greatly improve its enhancement effect; (3) The addition of pure MWCNTs in the polymer matrix enhanced the phonon scattering effect at the interface, which is related to the interface area.⁵⁵⁻⁵⁹ After surface modification, hydroxyl groups on the surface of BN nano-layer will greatly improve the dispersion of the BN-c-MWCNTs into the solvent or the polymer matrix, which is beneficial to the formation of thermal conductivity network, and therefore lower the content of the nano fillers.

However, the thermal conductivity enhancements of BN-c-MWCNTs to the polyimide matrices did not come up to expectation, and only showed comparable to that of Al(OH)-c-MWCNTs, which may be due to the polycrystalline structure

nature of the BN layer in this work. The control of crystal structure of BN layer by optimizing the preparation process is now undergoing in our group and the results will be reported later.

5 Conclusions

In summary, MWCNTs were successfully modified by an insulated inorganic BN nano-layer, and the layer thickness was about 3 nm. A series of thermally conductive insulated polyimide composites were successfully prepared by a two-step method. The BN layer can effectively prevent the formation of electrically conductive networks in the polyimide matrix. The values of surface and volume resistances of the BN-c-MWCNTs/PI films were around three orders of magnitude higher than those of the unmodified MWCNTs/PI when the MWCNTs content was 3 wt.%. The thermal conductive properties of the BN-c-MWCNTs/PI nano-composite films were obviously improved by low loadings of BN-c-MWCNTs, the thermal conductivity increased by about 106 % as compared with that of pure PI, and the enhancement was almost 5 times of that of MWCNTs/PI films. The BN-c-MWCNTs/PI films can be potentially used in the high-temperature microfabrication of heat dissipative components in the microelectronic industry because of their excellent thermal properties.

25 Acknowledgements

The financial support by the National 973 Program of China (2014CB643605 and 2011CB606100), the National Natural Science Foundation of China (51373204, 51173214, 51233008, J1103305), the Doctoral Fund of the Ministry of Education of China (20120171130001), Department of Education of Guangdong Province (2012KJCX0005), and the Science and Technology Bureau of Guangzhou (12C52051577) are gratefully acknowledged.

35 Notes and References

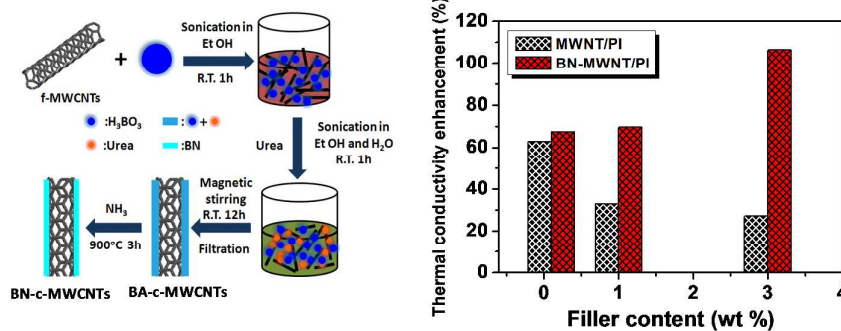
- 1 S. Iijima, *Nature*, 1991, **354**, 56-58.
- 2 Z. D. Han and A. Fina, *Prog. Polym. Sci.*, 2011, **36**, 914-944.
- 3 H. M. Duong, N. Yamamoto, K. Bui, D. V. Papavassiliou, S. Maruyama and B. L. Wardle, *J. Phys. Chem. C*, 2010, **114**, 8851-8860.
- 4 H. M. Duong, D. V. Papavassiliou, K. J. Mullen and S. Maruyama, *Nanotechnology*, 2008, **19**, 065702.
- 5 H. M. Duong, N. Yamamoto, D. V. Papavassiliou, S. Maruyama and B. L. Wardle, *Nanotechnology*, 2009, **20**, 155702.
- 6 J. W. Che, T. Cagin and W. A. Goddard, *Nanotechnology*, 2000, **11**, 65-69.
- 7 S. Shenogin, A. Bodapati, L. Xue, R. Ozisik and P. Keblinski, *Appl. Phys. Lett.*, 2004, **85**, 2229-2231.
- 8 B. L. Wardle, D. S. Saito, E. J. Garcia, A. J. Hart R.G. de Villoria and E. A. Verploegen, *Adv. Mater.*, 2008, **20**, 2707-2714.
- 9 A. P. Yu, P. Ramesh, X. B. Sun, E. Bekyarova, M. E. Itkis and R. C. Haddon, *Adv. Mater.*, 2008, **20**, 4740-4744.
- 10 T. L. Li and S. L. Chung Hsu, *J. Phys. Chem. B* 2010, **114**, 6825-6829.
- 11 S. H. Jin, K. H. Park, B. H. Kim, S. H. Hong and S. Jeon, *Small*, 2013, **9**, 2602-2610.
- 12 L. L. Chen, H. H. Ye, Y. Gogotsi, *J. Am. Ceram. Soc.*, 2004, **87**, 147-151.
- 13 Y. Zhang, S. X. Xiao, Q. Y. Wang, S. W. Liu, Z. P. Qiao, Z. G. Chi, J. R. Xu and J. Economy, *J. Mater. Chem.*, 2011, **21**, 14563-14568.
- 14 W. L. Wang, J. Q. Bi, W. X. Sun, H. L. Zhu, J. J. Xu, M. T. Zhao and Y. J. Bai, *Mater. Chem. Phys.*, 2010, **122**, 129-132.
- 15 J. B. Yoo, J. H. Han, S. H. Choi, T. Y. Lee, C. Y. Park, T. W. Jeong, J. H. Lee, S. G. Yu, G. S. Park, W. K. Yi, H. S. Kim, Y. J. Baik, J. M. Kim, *Physica B*, 2002, **323**, 180-181.
- 16 J. J. Ge, C. Y. Li, G. Xue, I. K. Mann, D. Zhang, F. W. Harris, S. Z. D. Cheng, S. C. Hong, X. Zhuang and Y. R. Shen, *J. Am. Chem. Soc.*, 2001, **123**, 5768-5776.
- 17 H. Lim, W. J. Cho, C. S. Ha, S. Ando, Y. K. Kim, C. H. Park and K. Lee, *Adv. Mater.*, 2002, **14**, 1275-1279.
- 18 G. W. Lee, M. Park, J. Kim, J. I. Lee and H. G. Yoon, *Composites A*, 2006, **37**, 727-734.
- 19 Y. Shimazaki, F. Hojo and Y. Takezawa, *ACS Appl. Mater. Interfaces.*, 2009, **1**, 225-227.
- 20 Y. Shimazaki, F. Hojo, and Y. Takezawa, *Appl. Phys. Lett.*, 2008, **92**, 133309-133311.
- 21 G. Droval, J. F. Feller, P. Salagnac and P. Glouanec, *Polym. Adv. Technol.*, 2006, **17**, 732-745.
- 22 P. Bujard, K. Kuhnlein, S. Ino and T. Shiobara, *IEEE Trans. Compon. Packag. Manuf. Technol. Part A*, 1994, **17**, 527-532.
- 23 W. S. Lee and J. Yu, 2005, **14**, 1647-1653.
- 24 P. Gonon, A. Sylvestre, J. Teyssyre and C. J. Prior, *Mater. Sci.: Mater. Electron.*, 2001, **12**, 81-86.
- 25 M. Hussain, Y. Oku, A. Nakahira, K. Niihara, *Mater. Lett.*, 1996, **26**, 177-184.
- 26 W. Zhou, C. Wang, T. Ai, K. Wu, F. Zhao, H. Gu, *Compos. Part A*, 2009, **40**, 830-836.
- 27 He, H.; Fu, R. Y. Shen, Y. Han and X. Song, *Compos. Sci. Technol.*, 2007, **67**, 2493-2499.
- 28 F. L. Riley, *J. Am. Ceram. Soc.*, 2000, **83**, 245-265.
- 29 J. Wang and X. S. Yi, *J. Appl. Polym. Sci.*, 2003, **89**, 3913-3917.
- 30 S. Yu, P. Hing and X. Hu, *Compos. Part A*, 2002, **33**, 289-292.
- 31 S. Kume, I. Yamada, K. Watari, I. Harada and K. Mitsuishi, *J. Am. Ceram. Soc.*, 2009, **92**, S153-S156.
- 32 E. S. Lee, S. M. Lee, D. J. Shanefield and W. R. Cannon, *J. Am. Ceram. Soc.* 2008, **91**, 1169-1174.
- 33 S. H. Xie, B. K. Zhu, Li, J. B. X. Z. Wei and Z. K. Xu, *Polym. Test.*, 2004, **23**, 797-801.
- 34 J. W. Bae, W. Kim, S. H. Cho and S. H. Lee, *J. Mater. Sci.*, 2000, **35**, 5907-5913.
- 35 K. C. Yung and H. Liem, *J. Appl. Polym. Sci.*, 2007, **106**, 3587-3591.
- 36 M. T. Huang, and Ishida, H. *J. Polym. Sci., Part B: Polym. Phys.*, 1999, **37**, 2360-2372.
- 37 W. H. Koh, *Components Technol. Conf.*, 1996, 343-346.
- 38 C. Harrison, S. Weaver, C. Bertelsen, E. Burgett, N. Hertel, E. Grulke, *J. Appl. Polym. Sci.*, 2008, **109**, 2529-2538.
- 39 H. Ishida and S. Rimdusit, *Thermochim. Acta*, 1998, **320**, 177-186.
- 40 R. F. Hill and P. H. Supancic, *J. Am. Ceram. Soc.*, 2002, **85**, 851-857.
- 41 T. H. Chiang and T. E. Hsieh, *J. Inorg. Organomet. Polym.*, 2006, **16**, 175-183.
- 42 W. Y. Zhou, S. H. Qi, Q. L. An, H. Z. Zhao and N. L. Liu, *Mater. Res. Bull.*, 2007, **42**, 1863-1873.
- 43 Y. Xu, D. D. L. Chung and C. Mroz, *Compos. Part A*, 2001, **32**, 1749-1757.
- 44 J. Zeng, R. Fu, Y. Shen, H. He and X. Song, *J. Appl. Polym. Sci.* 2009, **113**, 2117-2125.
- 45 J. Thomas, N. E. Weston, T. E. O'Connor, *J. Am. Ceram. Soc.*, 1963, **84**, 4619-4622.
- 46 T. R. Paine and C. K. Narula, *Chem. Rev.*, 1990, **90**, 73-91.
- 47 W. Zhou, P. Xiao, Y. Li and L. Zhou, *Ceram. Intl.*, 2013, **39**, 6569-6576.
- 48 V. Linss, S. Rodilb, P. Reinkec, M. Garnierd, P. Oelhafend, U. Kreissige and F. Richtera, *Thin Solid Films*, 2004, **467**, 76-87.
- 49 M. A. Mannan, M. Nagano, T. Kida, N. Hirao and Y. Baba, *J. Phys. Chem. Solids*, 2009, **70**, 20-25.
- 50 S. Y. Kim, J. Park, H. C. Choi, J. P. Ahn, J. Q. Hou and H. S. Kang, *J. Am. Chem. Soc.*, 2007, **129**, 1705-1716.
- 51 F. L. Huang, C. B. Cao, X. Xiang, R. T. Lv and H. S. Zhu, *Diamond Relat. Mater.*, 2004, **13**, 1757-1760.
- 52 Y. Zhang, X. X. Niu, X. F. Zheng, W. X. Lin, J. Z. Mai, Y. Z. Zhang, S. X. Xiao, S. W. Liu, Z. G. Chi, J. R. Xu, Faming Zhuanli Shengqing, 2009, CN 101575414 B.
- 53 Y. Zhang, X. X. Niu, X. F. Zheng, W. X. Lin, J. Z. Mai, Y. Z. Zhang, S. X. Xiao, S. W. Liu, Z. G. Chi, J. R. Xu, Faming Zhuanli Shengqing, 2009, CN 101600296 B.

-
- 54 S. Wang, Z. Liang, P. Gonnet, Y. H. Liao, B. Wang and C. Zhang,
Adv. Funct. Mater., 2007, **17**, 87-92.
- 55 P. C. Ma, S.Y. Mo, B. Z. Tang and J. K. Kim, *Carbon*, 2010, **48**,
1824-1834.
- 56 T. Zhou, X. Wang, X. Liu and D. Xiong, *Carbon*, 2010, **48**, 1171-
1176.
- 57 M. B. Bryning, M. F. Islam, J. M. Kikkawa and A. G. Yodh,
Adv. Mater., 2005, **17**, 1186-1191.
- 58 Y. F. Zhu, C. Ma, W. Zhang, R. P. Zhang, N. Koratkar and J. Liang, *J.*
Appl. Phys., 2009, **105**, 054319.
- 59 S. Choi, H. Im and J. Kim, *Nanotechnology*, 2012, **23**, 065303.

Graphical Abstract

Polyimide nanocomposites with boron nitride-coated multi-walled carbon nanotubes for enhanced thermal conductivity and electrical insulation

Wei Yan,^{ab} Yi Zhang,^{*a} Huawei Sun,^a Siwei Liu,^a Zhenguo Chi,^a Xudong Chen^a and Jiarui Xu^{*a}



Polyimide nanocomposites with boron nitride-coated multi-walled carbon nanotubes (BN-c-MWCNTs) were successfully prepared with enhanced thermal conductivity and electrical insulation.